Title
A case study of transport of tropical marine boundary layer and lower tropospheric air masses to the northern midlatitude upper troposphere

Journal
Journal of Geophysical Research, 105(D3)

ISSN
0148-0227

Authors
Grant, William B
Browell, Edward V
Butler, Carolyn F
et al.

Publication Date
2000-02-16

DOI
10.1029/1999jd901022

JOURNAL OF GEOPHYSICAL RESEARCH, VOL. 105, NO. D3, PAGES 3757-3769, FEBRUARY 16, 2000

A case study of transport of tropical marine boundary layer and lower tropospheric air masses to the northern midlatitude upper troposphere

William B. Grant,[1] Edward V. Browell,[1] Carolyn F. Butler,[2] Marta A. Fenn,[2] Marian B. Clayton,[2] John R. Hannan,[3] Henry E. Fuelberg,[3] Donald R. Blake,[4] Nicola J. Blake,[4] Gerald L. Gregory,[1] Brian G. Heikes,[5] Glen W. Sachse,[6] Hanwant B. Singh,[7] Julie Snow,[5] and Robert W. Talbot[8]

Abstract. Low-ozone (<20 ppbv) air masses were observed in the upper troposphere in northern midlatitudes over the eastern United States and the North Atlantic Ocean on several occasions in October 1997 during the NASA Subsonic Assessment, Ozone and Nitrogen Oxide Experiment (SONEX) mission. Three cases of low-ozone air masses were shown to have originated in the tropical Pacific marine boundary layer or lower troposphere and advected poleward along a warm conveyor belt during a synoptic-scale disturbance. The tropopause was elevated in the region with the low-ozone air mass. Stratospheric intrusions accompanied the disturbances. On the basis of storm track and stratospheric intrusion climatologies, such events appear to be more frequent from September through March than the rest of the year.

1. Introduction

There have been a number of observations of low-ozone air masses in the northern midlatitudes that have been traced to transport from the tropical marine boundary layer or lower troposphere. Table 1 gives a summary of a number of such observations, as well as some for which the source region was not identified. Since such data are generally reported during intensive field campaigns or other short-term measurement programs, they cannot be used to develop a climatology of low-ozone events. However, they do help establish that such transport does occur.

In addition, total ozone over central Europe has been studied as a function of weather pattern [*Kalvova and Halenka*, 1995; *Dubrovsky and Kalvova*, 1997]. The observation was made that when cyclonic weather patterns with northerly flow at 500 hPa existed, total ozone there was above normal 36.9% of the time, normal ozone 56.0% of the time, and below normal 7.1% of the time. When anticyclonic weather patterns with southerly flow existed, total ozone was below normal 28.5% of the time, normal 66.8% of the time, and above normal 4.7% of the time. When only flow direction was considered, above-normal total ozone was observed 30.1% of the time for northerly flow, while below-normal ozone was found 26.5% of the time for southerly flow.

The Subsonic Assessment, Ozone and Nitrogen Oxide Experiment (SONEX) mission provided an opportunity to obtain more information regarding the transport of low-ozone air from the tropics to northern midlatitudes. The purpose of SONEX was to study the upper troposphere/lower stratosphere in and near the North Atlantic flight corridor to better understand this region of the atmosphere and how civilian air travel might be affecting the atmospheric chemistry [*Singh et al.*, 1999]. Bases of operations included NASA Ames (Moffett Field), California (37.4°N, 122.1°W); Bangor, Maine (44.8°N, 68.8°W); Shannon, Ireland (52.7°N, 8.9°W); and Lajes, Terceira Island, Azores (38.8°N, 27.1°W). It took place from October 13 to November 12, 1997.

2. Low-Ozone Air Masses Observed on SONEX

Low-ozone air masses were observed on four flights during SONEX from October 13 to 23, 1997 (see Table 2). Plate 1 shows a pronounced example of low-ozone air in the upper troposphere, observed on the transit flight from NASA Ames Research Center to Bangor, Maine, on October 13. This atmospheric cross section of ozone was obtained using a combination of data from the NASA Langley Research Center's airborne UV differential absorption lidar (DIAL)

[1]Atmospheric Sciences Research, NASA Langley Research Center, Hampton, Virginia.
[2]Science Applications International Corporation, Hampton, Virginia.
[3]Department of Meteorology, Florida State University, Tallahassee.
[4]Chemistry Department, University of California, Irvine.
[5]Center for Atmospheric Chemistry Studies, Graduate School of Oceanography, University of Rhode Island, Narragansett.
[6]Aerospace Electronic Systems Division,NASA Langley Research Center, Hampton, Virginia.
[7]NASA Ames Research Center, Moffett Field, California.
[8]Institute for the Study of Earth, Oceans, and Space, University of New Hampshire, Durham.

Paper number 1999JD901022
0148-0227/00/1999JD901022$09 00

Table 1. Observations of Low-Ozone Air Masses Transported From the Tropical Marine Boundary Layer and Lower Troposphere to the Upper Troposphere at Northern Midlatitudes.

Dates	Latitude, Longitude	Altitude, km	Instrument	Ozone Concentration, ppbv	Authors
Midtroposphere					
Tropical source region, observed in Atlantic Ocean					
April 23, 1993	32.3°N, 64.8°W	11-12	ECC sonde	18	*Oltmans et al.* [1996]
July 12, 1996	52.4°N, 4.1°W	11-12	ECC sonde	2	Davies et al. [1998]
October 13-23, 1997	35°N-59°N, 9°W-92°W	6-15	UV DIAL	18	present study
Tropical source region, observed in Pacific Ocean					
March 4, 1994	27°N, 139°E	12-14.5	UV DIAL	<20	*Koike et al.* [1997]
August 11, 1993	35.4°N, 138.7°E	3.8	UV absorpt.	18	*Tsutsumi et al.* [1998]
Unknown source region					
May 2, 1993	38.8°N, 27.1°W	7-9*	ECC sonde	20-30	*Oltmans et al.* [1996]
May 29, 1997	47.5°N, 11.1°E	3-5#	UV DIAL	20-30	*Eisele et al.* [1999]
August 4, 27, 1993	32.3°N, 64.8°W	10-14*	ECC sonde	20-30	*Oltmans et al.* [1996]
Lower troposphere					
September 16, 1991	48°N, 133°E	1.5-2.5	UV DIAL		*Browell et al.* [1996]; *Merrill* [1996]
October 9, 1991	26.9°N, 128.3°E	0.02	UV absorpt.	20-25	*Akimoto et al.* [1996]

* no backward trajectory analyses were performed to determine whether the low ozone had come from the tropics.
\# backward trajectory calculations determined that the air mass came from 25°N, 60°W.

system [*Browell*, 1989; *Richter et al.*, 1997; *Browell et al.*, 1998] and in situ measurements [*Gregory et al.*, 1996] onboard the NASA DC-8. Values as low as 18 ppbv are evident in the middle of the low-ozone region. More typical ozone values for this time and place are 40-55 ppbv, as measured most of the time on the SONEX mission. A pronounced stratospheric intrusion is also evident just to the east of the Rocky Mountains. As will be discussed below, a synoptic-scale disturbance was associated with both the southerly transport of the tropical marine boundary layer (MBL) air and the descent of the stratospheric air. The elevated ozone in the lower troposphere between Pittsburgh, Pennsylvania, and Albany, New York, is attributed to photochemical smog [*Grant et al.*, 1998]. The Total Ozone Mapping Spectrometer (TOMS) image for that day (Plate 2) clearly shows high column ozone associated with a low tropopause near the Rocky Mountains and low column ozone associated with a high tropopause to the east of that. Figure 1 shows the UV DIAL/in situ tropospheric column ozone and the surface to 18 km column ozone as well as the tropopause height along the October 13 flight track. The tropopause height was calculated from the UV DIAL data, being the intersection of the tropospheric background ozone value with the trend in the stratospheric ozone. This generally occurs near a value of 100 ppbv. The ground to 18 km ozone column varies from 65 Dobson units (DU) outside the low-ozone air mass region to 20 DU inside. Note that 1 DU represents a milliatmosphere cm of ozone at 760 torr and 293 K.

The UV DIAL/in situ ozone profiles for October 15 and 20 were similar to that for October 13. The tropopause in the low-ozone region was near 15 km, and stratospheric air was observed on one or both sides down to 3-4 km, with the 100-ppbv contour dropping to 6 km on October 15 and 9 km on October 20. On October 23, only the latitudinal range 55°-58°N was sampled, and a 2-km layer of low ozone (22-40 ppbv) was found, along with occasional values as high as 65 ppbv in the 6-8 km region. The TOMS image for this day shows increased column ozone to the northeast of the flight track. The ozone column from the ground to 16 km for October 15 varied from 20 DU to 90 DU, while the ozone column from the ground to 17 km on October 20 varied from 8 DU to 70 DU.

Several approaches were used to verify that the low-ozone

Table 2. Parameters of Low-Ozone Observations and Comparisons During SONEX

Flight	Date	Latitude	Longitude	Altitude, km	Minimum O_3, ppbv	Negative PV*
3	Oct. 13	39°-46.5°N	92°-64°W	6-14	18	yes
4	Oct. 15	54°-55°N	60°-42°W	5-13	22	yes
6	Oct. 20	35°-43°N	9°-12°W	7-15	18	yes
7	Oct. 23	55°-59°N	9°W	9-12	22	no

*The values are just slightly negative.

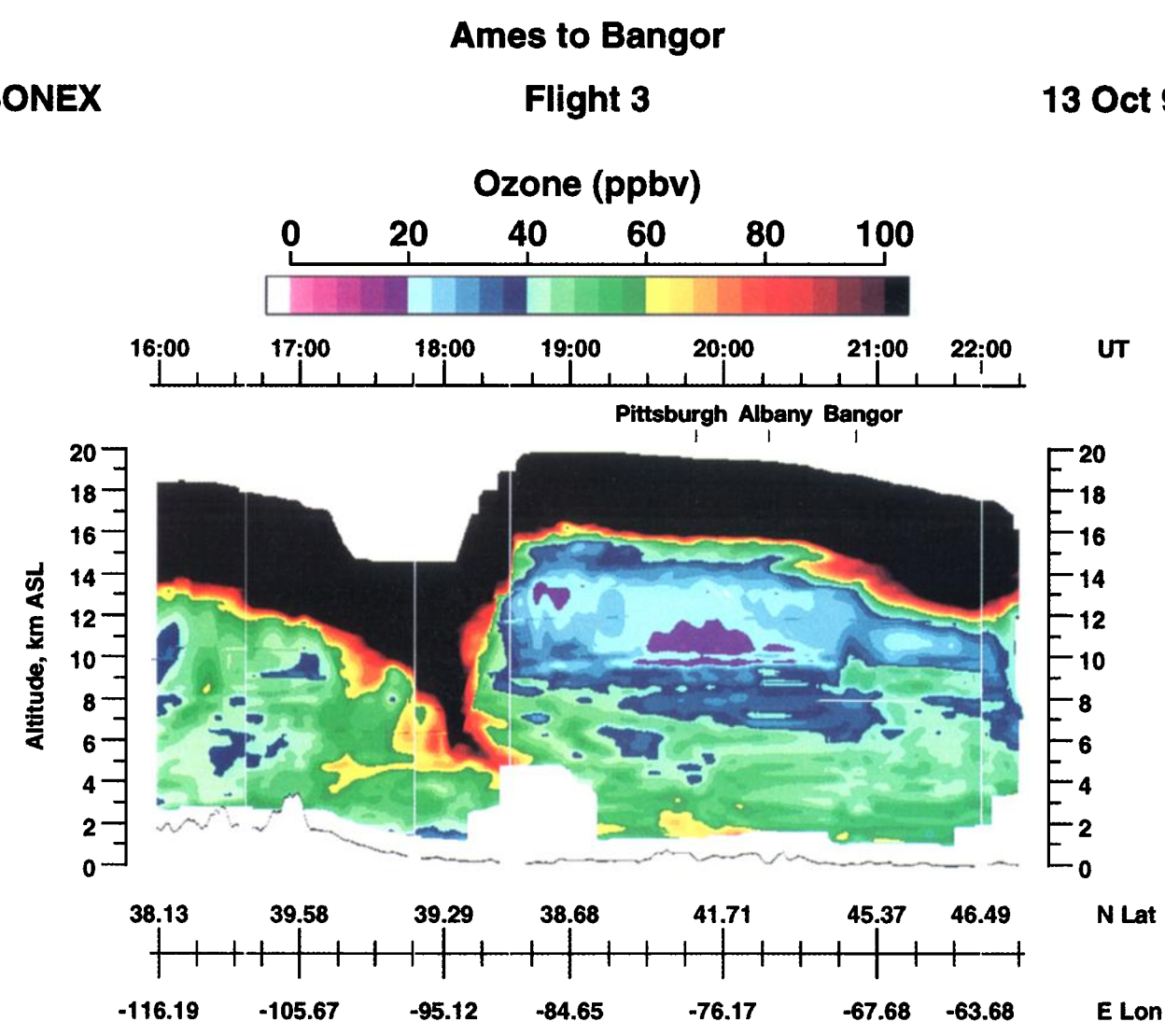

Plate 1. UV DIAL and in situ ozone data obtained on October 13, 1997, during the flight from NASA Ames, California, to Bangor, Maine. The vertical and horizontal resolutions are 300 m and 70 km, respectively, and the measurement precision/accuracy is 5 ppbv or 10%, whichever is larger. The black regions represent ozone in the stratosphere (concentration > 100 ppbv); the white regions indicate missing data. The dotted line at the bottom is the surface elevation. There is a stratospheric intrusion centered near 95°W.

air seen in northern midlatitudes originated in the tropical MBL: backward trajectory analysis; examination of potential vorticity levels; and comparison of molecular species concentrations found at midlatitude compared to the tropical MBL.

3. Backward Trajectories

Backward trajectories can be used to indicate where the air masses originated. Backward trajectory calculations were run at Florida State University using inputs from the European Centre for Medium-Range Weather Forecasts (ECMWF) in a kinematic analysis involving the u, v, and w components of the wind [*Fuelberg et al.*, 1996]. The ECMWF data are supplied with a horizontal resolution of 2.5° by 2.5° and 15 pressure levels in the vertical up to 100 hPa. The data are processed using a cubic spline procedure within the trajectory model in order to interpolate the data to equally spaced 5-hPa increments. Depending on the flight, 6-8 pressure levels somewhere in the range of 100 hPa to 400 hPa (flight 7), 500 (flight 6), 550 (flight 3), or 600 (flight 4) hPa were used. Data points were calculated each 15 minutes of flight time (~210 km). The backward trajectories went back 10 days, with an arrow indicating each day.

Figure 2 shows the backward trajectories calculated for flight 3 on October 13, 1997. All of the air masses along the flight track west of 70°W had origins equatorward of 20°N and at several pressure levels. The backward trajectories for arrival at 300 hPa all show ascent near 10°N, which is near the intertropical convergence zone (ITCZ), while at

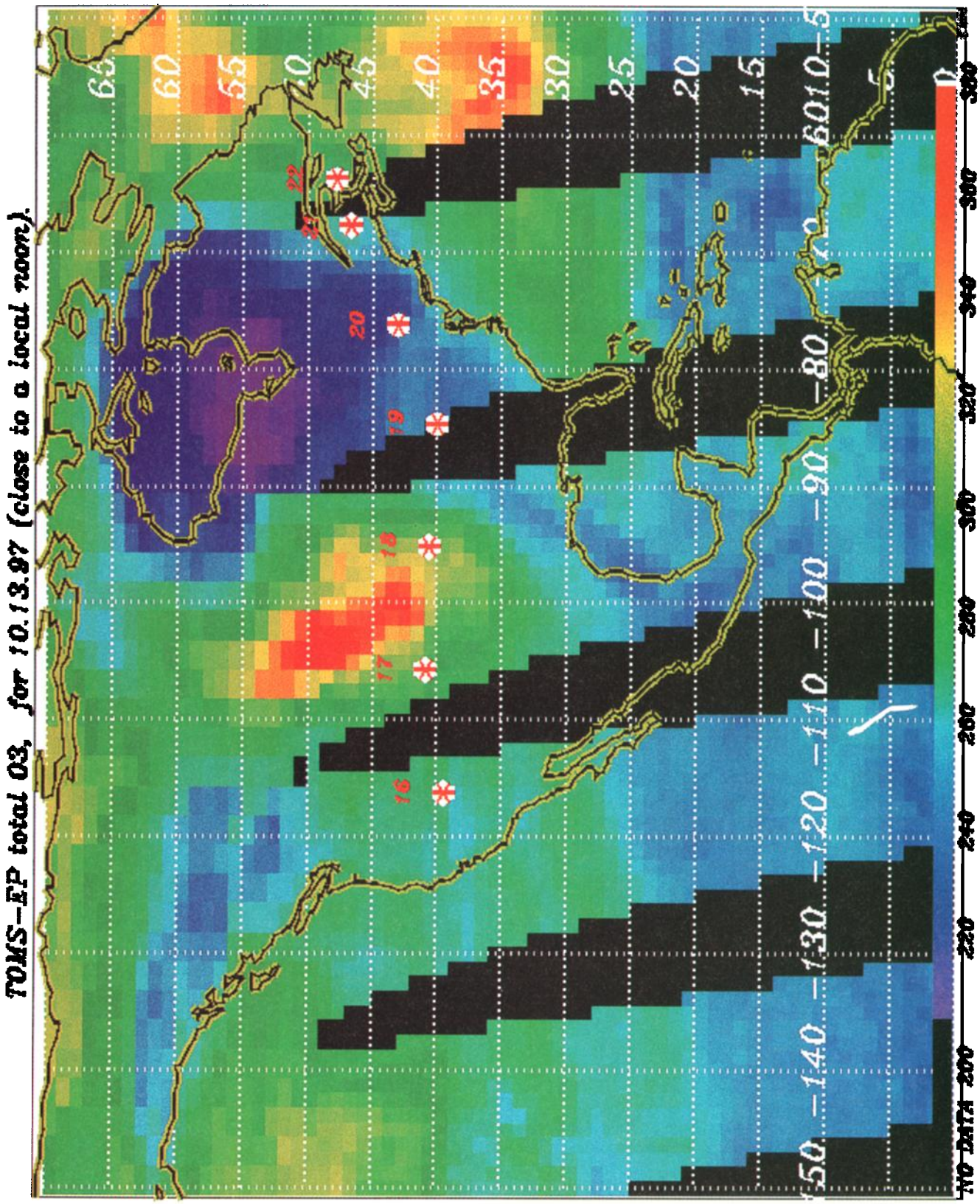

Plate 2. TOMS image for North America for October 13, 1997, for comparison with the UV DIAL data image.

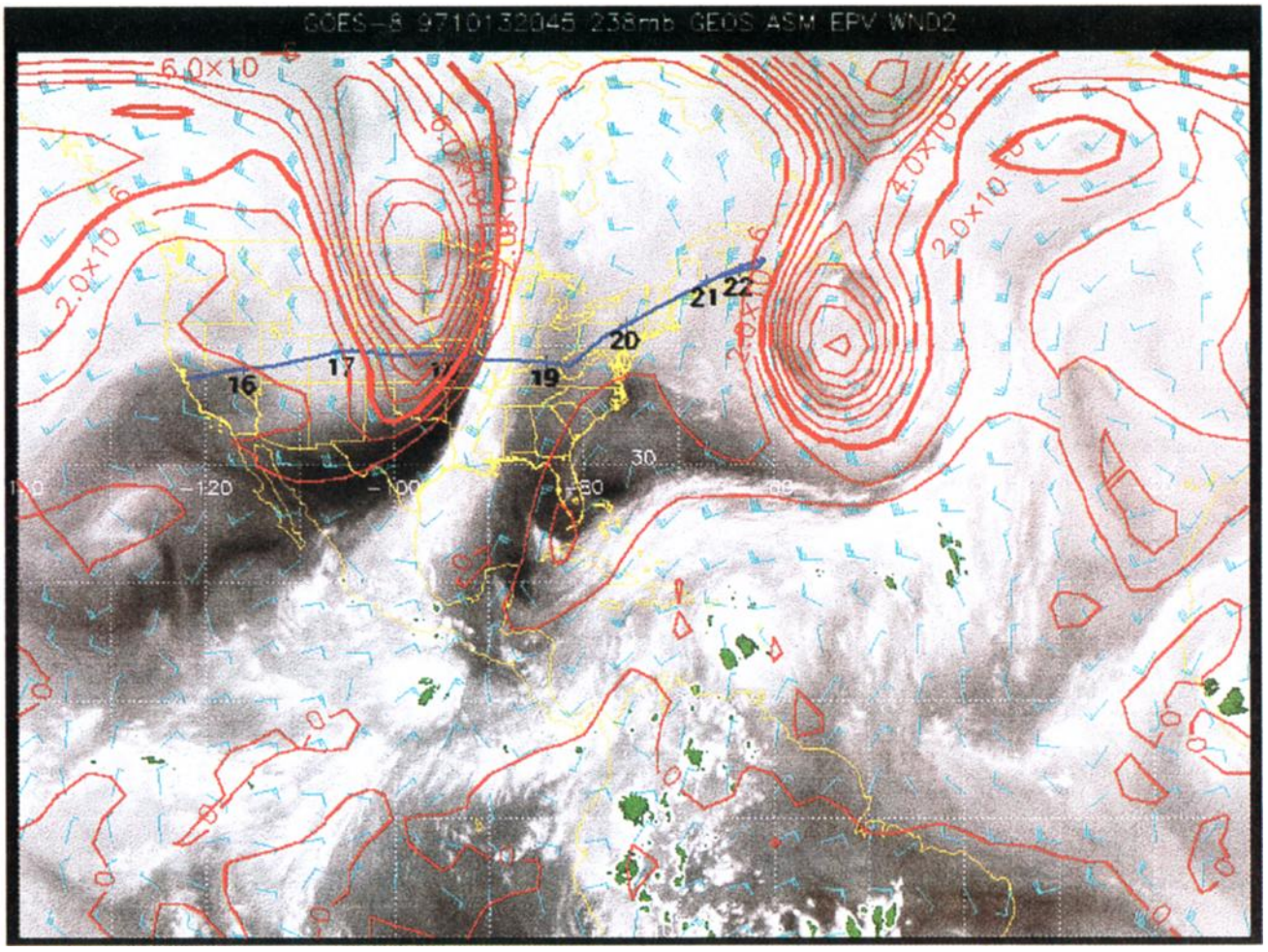

Plate 3. GOES-8 image for October 13, 1998, with PV model overlay.

< 150 hPa (not shown), there was generally descent. These backward trajectories along with the stratospheric intrusion shown in Plate 1 are consistent with the slantwise baroclinic motion which dominates midlatitude synoptic-scale disturbances. GOES-8 water vapor imagery for this day (Plate 3) shows an elongated band of cloudiness associated with the leading edge of a major trough-ridge system at approximately 90°W (1830 UT). The trough axis is characterized by confluence of descending dry stratospheric air to the west and ascending moist convective boundary layer air to the east [*Browning*, 1990]. The high ozone mixing ratios encountered at 10 km and 1800 UT are found within the dry stratospheric intrusion while the broadband of low-ozone mixing ratios encountered at 10 kilometers between 1900 and 2200 UT is found within the ascending air.

Cooper et al. [1998] also reported stratospheric air coming down to meet a "warm conveyor belt" (WCB). The GOES image in their Plate 1 clearly shows a WCB off the east coast of the United States with a cold front to the west of it. They found that stratospheric air was generally found behind a cold front, but not ahead of the front. *Harrold* [1973] presented an early analysis of the WCB. Such WCBs typically have a width of 100-1000 km, a depth of a few km, and initially flows parallel to and in advance of a surface cold front. Precipitation is also formed in an extensive midtropospheric flow.

The injection of ozone-rich air into the troposphere via stratospheric intrusions has been extensively studied [*Danielsen and Mohnen*, 1977; *Danielsen*, 1980; *Browell et al.*, 1987]. *Danielsen and Mohnen* [1977] state that ozone-rich air is transported into the troposphere with each major cyclonic development.

However, the transport of ozone-poor air from the convective boundary layer into the upper troposphere via the WCB has received less attention [*Bethan et al.*, 1998]. This transport occurs along the WCB of northward moving, saturated air which lies ahead of the confluence line in mature mid-latitude disturbances. The southern end of the WCB lies within the convective boundary layer while the northern end extends into the upper troposphere. Latent heat release associated with frontal precipitation results in diabatic ascent of the saturated boundary layer air along surfaces of constant equivalent potential temperature. On October 13 the WCB extends from Baja California (20°N) to central Ontario (55°N) (see Plate 3). The origin of the low-ozone mixing ratios shown in Plate 1 is likely to be within the convective boundary layer at the southern end of the WCB.

Most of the backward trajectories for flight 4, October 15, originated equatorward of 20°N, this time associated with a strong convective updraft associated with the 300-hPa air mass 5 days prior to arrival, followed by more gradual

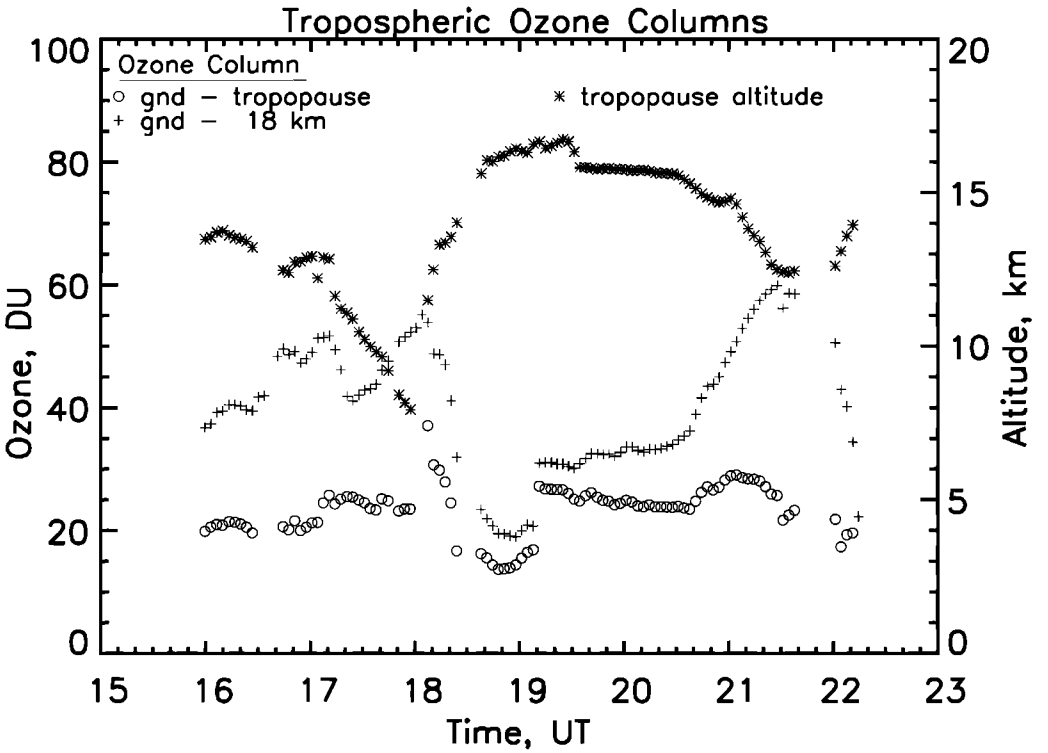

Figure 1. Tropospheric ozone columns and tropopause height determined by the UV DIAL/in situ instruments onboard the DC-8 for the SONEX October 13, 1997 flight.

ascents. For flight 6, October 20, some of the flight tracks originated below 20°N, while for flight 7, October 23, only a few of the backward trajectories had such origins.

4. Potential Vorticity (PV)

Potential vorticity can also be used to help identify the origin of the low-ozone air masses. As shown by *Browell et al.* [1987, 1996], *Beekmann et al.* [1994], *Newell et al.* [1997], *Fenn et al.* [1999], and references therein, there is a high correlation between the PV and ozone of stratospheric origin in the troposphere. Both PV and ozone are well conserved in the lower stratosphere. However, the correlation decreases at lower altitudes in the troposphere [*Beekmann et al.*, 1994]. Plate 3 has PV model products overlaid on the GOES-8 image, clearly showing that the two high-column-ozone regions in the TOMS image were related to high PV at 238 hPa. In addition, since the sign of PV changes from positive in the northern hemisphere (NH) to negative in the southern hemisphere (SH), any finding of negative PV would also be indicative of transport from the tropics to northern midlatitudes. In fact, some transport of air masses from the NH to SH was found in the Pacific Exploratory Mission-Tropics A (PEM-Tropics A) data set [*Fenn et al.*, 1999]. For SONEX, several flights including that of October 13 showed negative values of PV (see Table 2). Modified PV cited here was from the Goddard Space Flight Center/Data Assimilation Office (GSFC/DAO) assimilation model [*Thompson et al.*, 1999].

5. Concentrations of Molecular Species

Ozone mixing ratios in the tropical MBL are low, on the order of 5-20 ppbv [*Routhier et al.*, 1980; *Browell et al.*, 1996; *Singh et al.*, 1996; *Newell et al.*, 1997; *Browell et al.*, 1998; *Fenn et al.*, 1999]. This is due to net ozone destruction resulting from photolysis of ozone and water vapor during high UV irradiance and the production of peroxy radicals through reactions with carbon monoxide or methane in an atmosphere low in precursors for ozone formation [*Thompson et al.*, 1993; *Monks et al.*, 1998].

Concentrations of other trace species can provide additional evidence that the low-ozone air masses observed in northern midlatitudes had tropical MBL origins. The PEM-Tropics A data set (southern Pacific from August 30 to October 6, 1996) [*Fenn et al.*, 1999] includes trace species concentrations in the tropical MBL. The category of near-surface (NS) air includes data obtained within 3 km of the ocean surface, with about half of the data coming from the tropics and the other half from southern mid and high latitudes. Another category called reference (REF) includes data which are within 20% of the reference ozone profile and did not have high aerosol loading. It did not include data from the MBL. The values for the NS and REF cases are included in Table 3. Some comments can be made about the agreement between the PEM-Tropics A NS and SONEX low-ozone air masses. The three short-lived (2 days) ocean source species, CH_3I, $CHBr_3$, and CH_3Cl, had the best agreement with the SONEX values, as might be expected for rapid transport from the tropics to midlatitudes. The peroxides concentrations were much lower in SONEX than in PEM-Tropics A, which is reasonable since they are water-soluble. The other species for which comparisons can be made had higher concentrations for SONEX than for PEM Tropics-A. Peroxyacetyl nitrate (PAN), which has a high source in the stratosphere, was much higher in SONEX air masses than in PEM-Tropics A NS air masses, suggest-

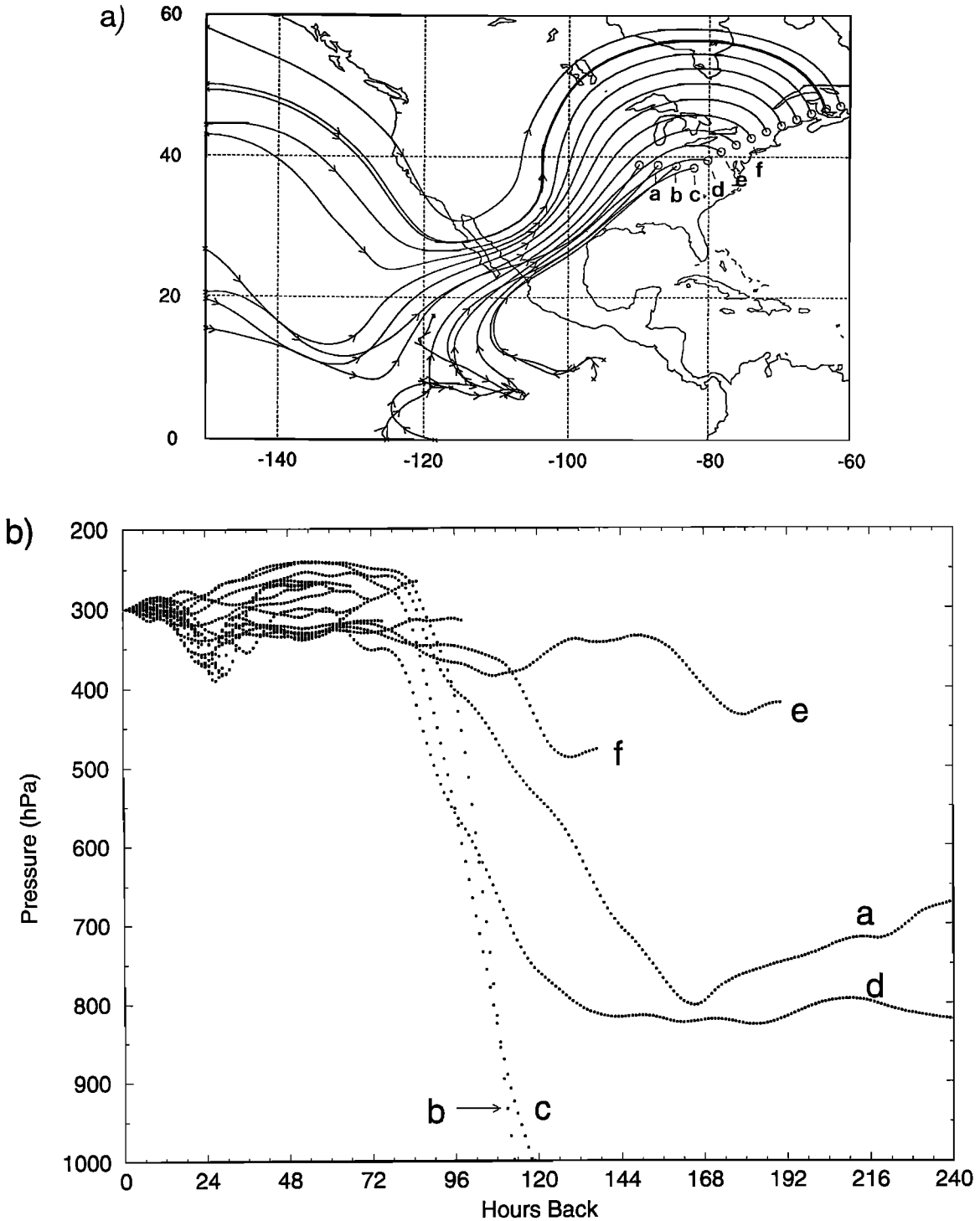

Figure 2. (a) Backward trajectories for flight 3, October 13, 1997, at 300 hPa (9.2 km) showing that much of the air mass sampled had origins in the tropical Pacific Ocean. (b) Same as 1a, but showing the vertical motion of the air masses.

ing that there was significant mixing from mid and upper troposphere in the SONEX air masses.

Comparisons can also be made with data from NS and background air masses from PEM-West A [*Browell et al.*, 1996]. The PEM-West A values were sometimes higher and sometimes lower than the PEM-Tropics A values.

Bethan et al. [1998] also measured concentrations of trace species in an air mass transported from the subtropical MBL to northern midlatitudes. They obtained bottle samples as well as measuring CO, NO, and NO_x at 46.4°N, 10.6°W for an aircraft altitude of 4 km. Their values, reported in their Tables 1 and 2, while lower for short-lived species than the adjacent air mass, are generally much higher than observed during SONEX. This suggests that the air masses reported by Bethan et al. may have already mixed with preexisting mid-latitude air.

Table 3. Trace Species Concentrations (5-min Merged Data) Measured in the Tropical Air Masses Transported to Northern Midlatitude Compared With Measurements Made in the Near-Surface Layer During PEM-West A [*Browell et al.*, 1996] and PEM Tropics-A [*Fenn et al.*, 1999]

Parameter / Date	Flight 3 October 13	Flight 4 October 15	Flight 4 October 15	Flight 6 October 20	SONEX Flight 7 October 23	Flight 7 October 23	Average	PWA NS*	REF*	PWA NS	BKG*
Time, s	71,100	46,200	48,900	40,200	32,100	33,900					
Latitude, °N	40.7	48.7	53.4	34.0	58.1	55.3					
Longitude, °W	78.3	65.8	59.6	13.1	9.0	9.1					
Pressure altitude, km	11.3	10.0	9.1	11.3	10.6	11.2	10.6±0.8				
Water H_2O, ppm	92.7	194	673	143	134	87.5	221±205				
O_3, ppb	21.3	32.6	33.0	26.2	28.8	29.1	28.5±4.0 12.8	42.9	20.5	42.4	
Peroxides (short-lived)											
H_2O_2, ppt	146.7	158.4	255.0	106.7	175.6	132.0	162.4±46.6	1562	566	1012	423
CH_3OOH, ppt	54.2	110.6	65.5	207.5	55.0	85.2	96.3±53.4	1419	272	861	267
Anthropogenic sources [Simpson et al., this issue]											
C_2HCl_3, ppt	0.195	0.171	0.149	0.088	0.066	0.097	0.128±0.047				
$CHCl_3$, ppt	6.13	7.05	7.24	6.19	6.19	6.32	6.52±0.45				
C_2Cl_4, ppt	2.35	3.62	3.48	2.33	2.20	2.86	2.81±0.57	3.58	3.92	1.40	1.28
H1301, ppt	2.295	2.419	2.366	2.320	2.440	2.360	2.367±0.051				
F11, ppt	260.2	263.6	264.1	259.6	260.7	262.0	261.7±1.7				
Combustion source species											
C_2H_2, ppt	26.4	92.1	72.5	45.6	57.5	52.0	57.7±20.7	73.7	56.5	36.8	52.5
C_2H_6, ppt	352	696	711	577	584	614	589±118 507	492	295	349	
Natural + lesser anthropogenic source including combustion											
CO, ppb	64.1	84.0	78.6	74.7	78.3	x	75.9±6.6 92.5	76.3	58.3	62.3	
CH_4, ppm	1725	1753	1743	1742	x	x	1741±10 1718	1724	1697	1705	
Ccean source species											
CH_3I, ppt	0.19	0.32	0.33	0.27	0.23	0.18	0.25±0.06			0.34	0.07
$CHBr_3$, ppt	0.61	1.62	1.69	0.73	0.48	0.57	0.95±0.50			1.25	0.46
CH_3Cl, ppt	537.2	573.8	564.5	538.7	532.4	536.3	547.2±15.9			549	563
High sources in stratosphere											
HNO_3, ppt	21.5	21.5	55.0	38.4	120.8	39.2	49.4±33.9			20.1	65.8
PAN, ppt	6.1	62.2	65.7	12.7	24.8	21.0	32.1±23.3	2.0	45.5	3.0	44.5
Miscellaneous											
$MeNO_3$, ppt	8.66	4.93	4.80	3.35	3.71	4.80	5.04±1.73				
Acetone, ppt	257	713	521	608	564	566	538±139				

* NS, near surface; REF, reference; BKG, background; PTA, PEM-Tropics A; PWA, PEM-West A.

6. Synthesis

Thus, three ways were used to check that the low-ozone air seen in northern midlatitudes originated in the tropical Pacific MBL: backward trajectories; PV analysis; and concentrations of trace species in comparison with those found earlier in the tropical MBL. Backward trajectory calculations and PV could each be used independently to determine the presence of tropical MBL air in the northern mid-latitude upper troposphere. Concentrations of trace species was most useful for ocean source species with short residence times, CH_3I, $CHBr_3$, and CH_3Cl. Together, the three approaches make an strong case that the air masses came from the tropical Pacific Ocean with the tropical MBL properties intact.

7. Climatologies Related to Low-Ozone Transport From the Tropical MBL and Lower Troposphere

7.1. Ozonesonde Results

Ozonesondes can be used to provide climatological data regarding the occurrence of low ozone in the northern midlatitudes. *Austin and Follows* [1991] used the 20-year ozonesonde record at Payerne, Switzerland, finding that the frequency of stratospheric intrusions at 300 hPa was maximized in late winter/early spring and minimal during the summer. *Beekmann et al.* [1994] provided tropospheric ozone climatologies using Brewer-Mast ozonesonde data for the Observatorie de Haute Provence, southern France (44°N, 6°E). The ozone in the 5-10-km region was lowest during October-March, dropping below 40 ppbv on average, compared with over 60 ppbv during the middle of the year. Similar results were shown for other European ozonesonde stations. Also, the height of the 120 ppbv contour was shown to be highest from September though November, rising above 12 km.

Oltmans et al. [1996] provide ozonesonde data plots for several stations in the Atlantic Ocean from 32°N to 65°N in the early 1990s. The only low-ozone occurrences of note are presented in Table 1. A tropical source was indicated by backward trajectories for the April 23, 1993 Bermuda data [*Oltmans et al.*, 1996].

The electrochemical concentration cell (ECC) ozonesonde data for Wallops Island, Virginia (37.5°N/75.3°W) for the period January 5, 1979 to December 22, 1992 [*Pierce and Grant*, 1998; *Thouret et al.*, 1998] were also reprocessed to develop a climatology of low-ozone air masses over a point in the eastern United States. The Wallops Island ozonesondes were used since there is a long period of continuous measurements, and since it represents northern continental midlatitudes. A total of 425 ozonesondes were used in the study. Figure 3 shows the mean ozone mixing ratio below the actual tropopause with the data averaged monthly, as well as the frequency of ozone excesses and deficits greater than 30% from the monthly mean. The 100-ppbv contour line is lower during the middle of the year than at the end of the year, and is significantly below the mean tropopause height in the middle of the year, but above it at the end of the year. The period from April to September has the highest ozone values while the period from September to April or May has the highest variability [see also *Thouret et al.*, 1998]. Thus the SONEX period occurred during a time with about average variability. Note that most of the ozone excess and deficit cases occur within 2-4 km of the seasonal average tropopause height. This is consistent with the ozone distribution shown in Plate 1 in which a synoptic-scale disturbance involves both a stratospheric intrusion and long-range transport of low-ozone air from the tropical MBL.

7.2. Storm Track Climatologies

Storm track climatologies can also be used to suggest when WCB transport of tropical MBL air to northern midlatitudes might occur. *Blackmon et al.* [1977] provided an early analysis of NH Atlantic and Pacific Ocean storm tracks, which generally occur during fall and winter. *Hoskins and Valdes* [1990] point out that the warm oceans off the east coasts of the cold North American and Asian continents provide the conditions in which winter storm tracks are inevitable. However, such conditions are lacking in the SH so storm tracks are more extended (130° in longitude over the Atlantic) and less definite [*James and Anderson*, 1983].

Chang [1999] examined the characteristics of wave packets in the upper troposphere for seasonal and hemispheric variations. The 300-hPa zonal wind was much higher in the NH in winter (>60 m s^{-1}) than summer (>20 m s^{-1}), and standard deviations of the 300-hPa v' for 1980-1993 was high in the NH in winter, with the highest values extending from the mid Pacific Ocean to northern Europe. Meridional group velocities were much higher in the NH for winter than for summer. This analysis also supports winter as having more tropospheric poleward transport than summer.

7.3. Stratospheric intrusion climatologies

Since the three long flight track observations of upper tropospheric low ozone masses transported from the tropics occurred in conjunction with stratospheric intrusions, it seems that such coupling may be frequent. This assumption is supported by *Danielsen and Mohnen* [1977]. Thus the climatology of stratospheric intrusions is a second area of investigation.

Cooper et al. [1998] reviewed a number of studies on stratosphere intrusions, finding that most of the papers reported a higher frequency of stratospheric intrusions in the fall-to-spring period in the NH. *Johnson and Viezee* [1981] found ozone intrusions in virtually every trough that they sampled over the central United States in the fall and spring of 1978. *Beekmann et al.* [1997] reported the seasonal variation of stratospheric air injections at the Zugspitze (2964 m above sea level (asl)) and Wank (1780 m asl) mountain stations in Germany. During the period from September to April, Wank had a high number of events per month (7-12 per month, median equal to 8) as did Zugspitze (13-28 per month, median equal to 17), while during the period May to August, Wank had a low number (1-4 per month), while Zugspitze had a moderate number (9-15 per month).

Beekmann et al. [1997] also show the distribution of the annual mean distribution of the global tropopause folding activity for 1984-1993 with a 10° grid spacing. The loca-

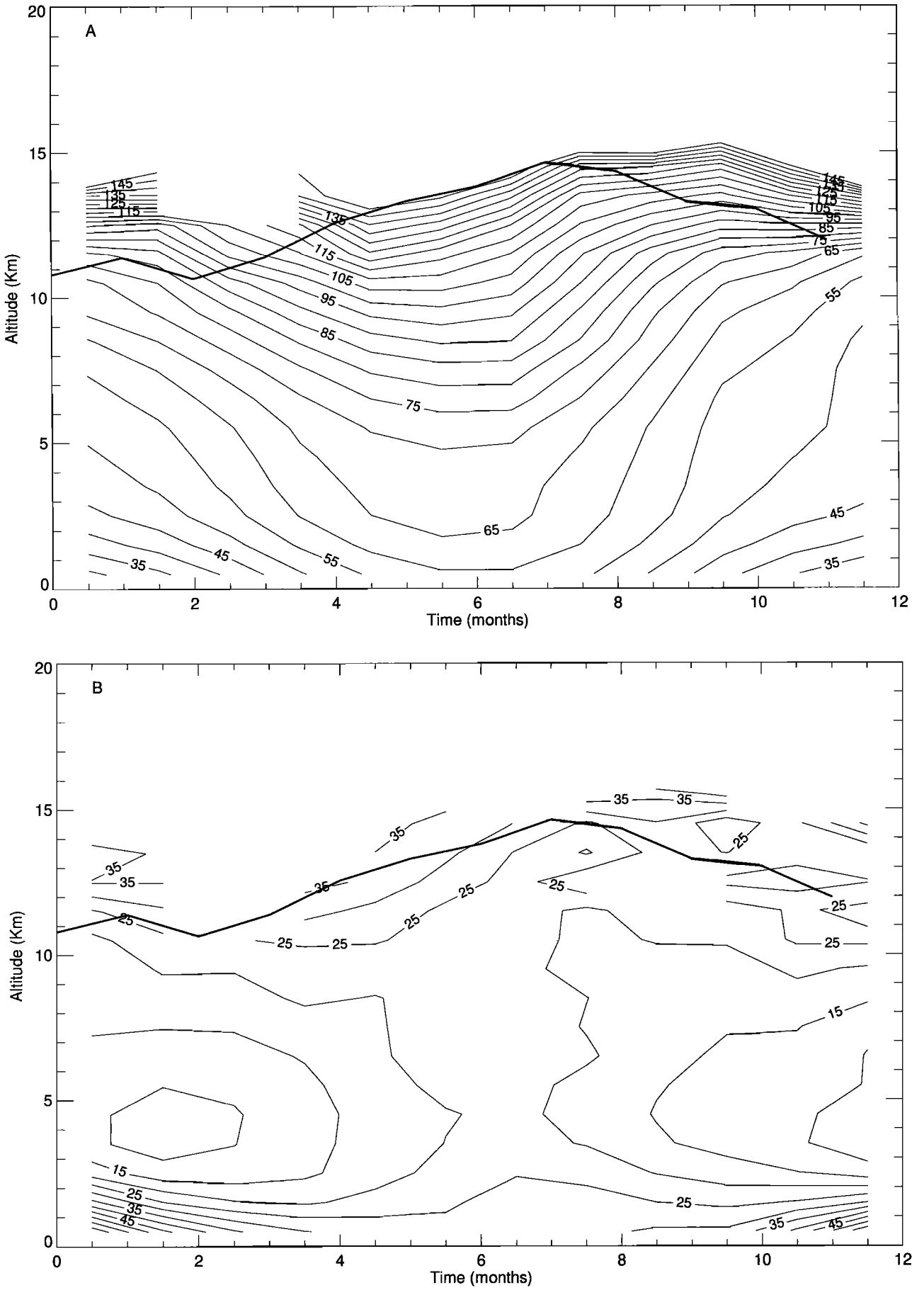

Figure 3. (a) The mean ozone mixing ratio below the actual tropopause with the data averaged monthly using ECC ozonesondes for Wallops Island, Virginia. The dark line is the monthly mean tropopause height. (b) The frequency of ozone excesses >30% above the monthly mean. (c) The frequency of ozone deficits <30% below the monthly mean.

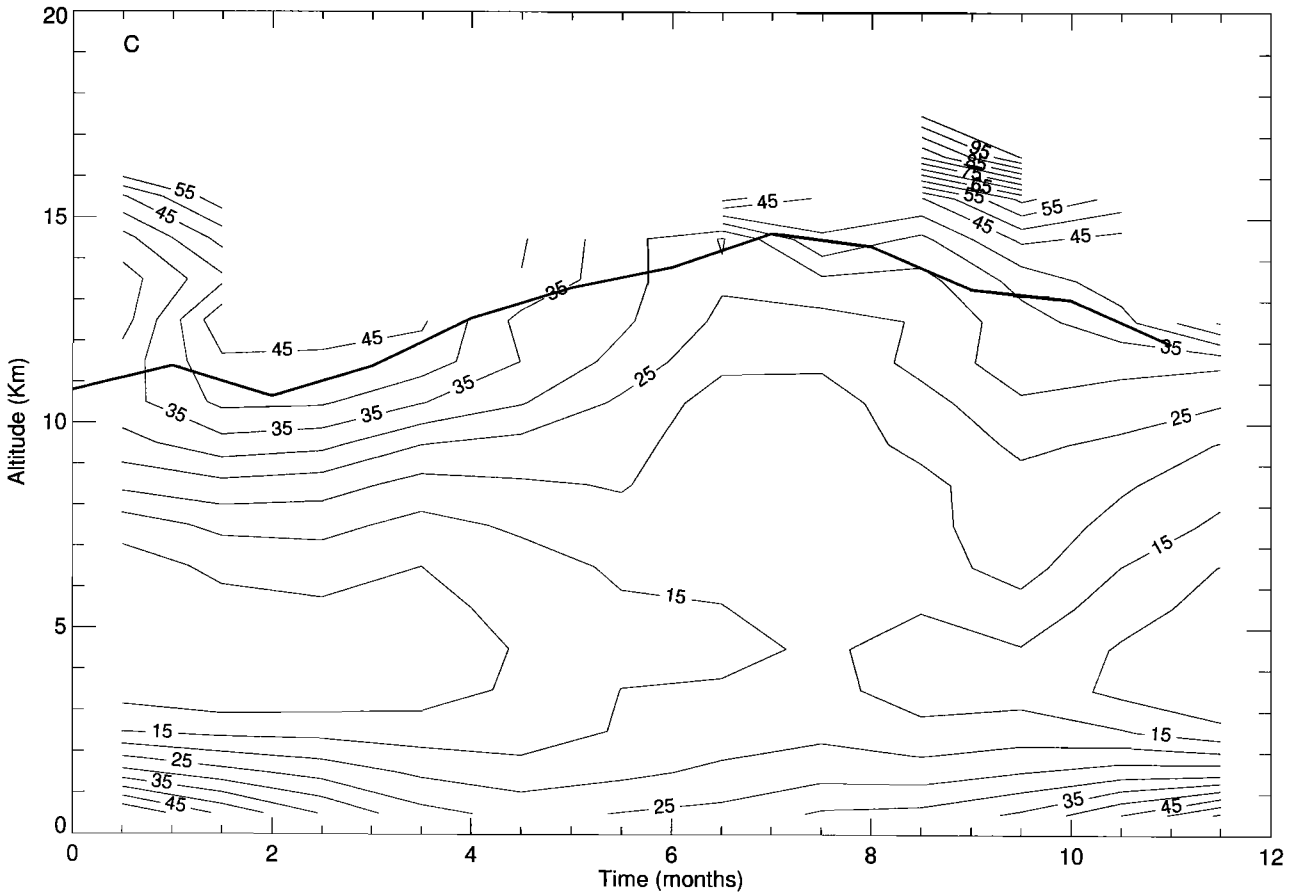

Figure 3. (continued)

tions with >50 events/year in the NH are found primarily from eastern North America to central Europe poleward of about 35°, with a few more south of Alaska but north of 50°. The region of eastern Asia from 35°-55°N had >40 events/year. In general, the oceans had more events/year than did the continents. The locations of the higher frequencies of tropospheric folding activity generally correspond to the locations of high storm track activity.

While there are a number of cases where stratospheric intrusions were associated with WCB transport from the tropics to midlatitudes, the two processes are not necessarily linked. In general, the WCB is associated with a mature midlatitude cyclone or synoptic-scale disturbance. The WCB is situated ahead of a cold front. Stratospheric intrusions are associated with jet streaks, which may or may not be coupled to the midlatitude cyclones.

8. Summary and conclusion

Low-ozone air masses were found in the upper troposphere of northern midlatitudes between 13.1°W and 91.1°W on four flights during the SONEX mission in October 1997. Using a variety of techniques, such as backward trajectory calculations, PV analysis, and concentrations of various species, it was shown that these air masses have origins in the tropical MBL. Convective lofting near the ITCZ may be involved in moving the MBL air to higher altitudes, but evidently is not required. The synoptic-scale weather patterns involving WCB can transport the air mass to midlatitude upper troposphere. Stratospheric intrusions were found to be associated with the WCB transport and appear to be generally coupled to WCB transport in such synoptic-scale disturbances.

Future work to more firmly establish the climatology of transport from the tropical MBL to northern midlatitudes might involve the use of TOMS daily global total ozone maps, GOES water vapor images and wind fields. In addition, PV contour maps could be used to establish the link with stratospheric intrusions. A preliminary inspection of TOMS images indicates that coupled low/high ozone dipoles in which the low-ozone region moves from the tropics poleward in a northeasterly direction and eventually dissipate are fairly frequent in the September-March period.

Acknowledgments. The authors thank A. Notari (SAIC), L. W. Overbay, W. J. McCabe, and J. A. Williams for technical support of the UV DIAL system during SONEX. The authors also thank M. A. Owens (Hampton University), A. M. Thompson (NASA Goddard Space Flight Center), and two anonymous referees for helpful comments on the manuscript. The authors thank R. B. Pierce for the Wallops ozonesonde data analysis, A. D. Frolov (University of Maryland) for the TOMS image, and L. Pfister (NASA Ames Research Center), T. L. Kucsera (Steven Myer and Associates, Corp. at NASA Goddard Space Flight Center) and A. M. Thompson for the GOES-8 image.

References

Akimoto, H., et al., Long-range transport of ozone in the East Asian Pacific rim region, *J. Geophys. Res.*, *101*, 1999-2010, 1996.

Austin, J. F., and M. J. Follows, The ozone record at Payerne: an assessment of the cross-tropopause flux, *Atmos. Environ. Part A, 25*, 1873-1880, 1991.

Beekmann, M., G. Ancellet, and G. Megie, Climatology of tropospheric ozone in southern Europe and its relation to potential vorticity, *J. Geophys. Res., 99*, 12,841-12,853, 1994.

Beekmann, M., et al., Regional and global tropopause fold occurrence and related ozone flux across the tropopause, *J. Atmos. Chem., 28*, 29-44, 1997.

Bethan, S., G. Vaughan, C. Gerbig, A. Volz-Thomas, H. Richer, and D. A. Tiddeman, Chemical air mass differences near fronts, *J. Geophys. Res., 103*, 13,413-13,434, 1998.

Blackmon, M. L., J. M. Wallace, N.-C. Lau, and S. L. Mullen, An observational study of the Northern Hemisphere winter-time circulation, *J. Atmos. Sci., 34*, 1040-1053, 1977.

Browell, E. V., Differential absorption lidar sensing of ozone, *Proc. IEEE, 77*, 419-432, 1989.

Browell, E. V., et al., Tropopause fold structure determined from airborne lidar and in situ measurements, *J. Geophys. Res., 92*, 2112-2120, 1987.

Browell, E. V., et al., Large-scale air mass characteristic observed over western Pacific during summertime, *J. Geophys. Res., 101*, 1691-1712, 1996.

Browell, E. V., S. Ismail, and W. B. Grant, Differential absorption lidar (DIAL) measurements from air and space, *Appl. Phys. B 67*, 399-410, 1998.

Browning, K. A., Organization of Clouds and Precipitation in *Extratropical Cyclones, Extratropical Cyclones: The Erik Palmen Memorial Volume*, edited by C. W. Newton and E. O. Holopainen, Am. Meteorol. Soc., pp. 129-153, Boston, Mass., 1990.

Carroll, M. A., et al., Aircraft measurements of NO_x over the eastern Pacific and continental United States and implications for ozone production, *J. Geophys. Res., 95*, 10,205-10,233, 1990.

Chang, E. K. M., Characteristics of wave packets in the upper troposphere. Part II: Seasonal and hemispheric variations, *J. Atmos. Sci., 56*, 1729-1747, 1999.

Cooper, O. R., J. L. Moody, J. C. Davenport, S. J. Oltmans, B. J. Johnson, X, Chen, P. B. Shepson, and J. T. Merrill, Influence of springtime weather systems on vertical ozone distributions over three North American sites, *J. Geophys. Res., 103*, 22,001-22,013, 1998.

Danielsen, E. F., Stratospheric source for unexpectedly large values of ozone measured over the Pacific Ocean during Gametag, August 1977, *J. Geophys. Res., 85*, 401-412, 1980.

Danielsen, E. F., and V. A. Mohnen, Project Duststorm Report: Ozone Transport, in Situ Measurements, and Meteorological Analysis of Tropopause Folding, *J. Geophys. Res., 82*, 5867-5877, 1977.

Davies, W. E., G. Vaughan, and F. M. O'Connor, Observation of near-zero ozone concentrations in the upper troposphere at mid-latitudes, *Geophys. Res. Lett., 25*, 1173-1176, 1998.

Dubrovsky, M., and J. Kalvova, The daily total ozone: the mean annual cycle and correlation with meteorological conditions, in *Atmospheric Ozone, Proceedings of XVIII Quadrennial Ozone Symposium, vol. 1, L'Aquila, Italy, 12-21 September 1996*, edited by R. D. Bojkov and G. Visconti, pp. 33-36, World Meteorol. Org., Geneva, 1997.

Eisele, H., H. E. Scheel, R. Sladkovic, and T. Trickl, High-resolution lidar measurements of stratosphere-troposphere exchange, *J. Atmos. Sci., 56*, 319-330, 1999.

Fenn, M. A., et al., Ozone and aerosol distributions and air mass characteristics over the South Pacific during the burning season, *J. Geophys. Res., 104*, 16,197-16,212, 1999

Fuelberg, H. E., R. O. Loring Jr., M. V. Watson, M. C. Sinha, K. E. Pickering, A. M. Thompson, G. W. Sachse, D. R. Blake, and M. R. Schoeberl, TRACE A trajectory intercomparison, 2, Isentropic and kinematic methods, *J. Geophys. Res., 101*, 23,-927-23,939, 1996.

Grant, W. B., C. F. Butler, M. A. Fenn, S. A. Kooi, E. V. Browell, and H. Fuelberg, Chemistry and dynamics of the lower troposphere over North America and the North Atlantic Ocean in fall 1997 observed using an airborne UV DIAL system, in *Abstracts of the Nineteenth International Laser Radar Conference, Annapolis, Maryland, July 6-10, 1998*, edited by U. N. Singh, S. Ismail, and G. K. Schwemmer, NASA Langley Research Center, Hampton, Virginia, pp. 379-381, 1998.

Gregory, G. L., B. E. Anderson, and E. V. Browell, Influence of lower tropospheric ozone on total column ozone as observed over the Pacific Ocean during the 1991 PEM-West A expedition, *J. Geophys. Res., 101*, 1919-1930, 1996.

Harrold, T. W. Mechanisms influencing the distribution of precipitation within baroclinic disturbances, *Q. J. R. Meteorol. Soc., 99*, 232-251, 1973.

Hoskins, B. J., and P. J. Valdes, On the existence of storm-tracks, *J. Atmos. Sci., 47*, 1854-1864, 1990.

James, I. N., and D. L. T. Anderson, The seasonal mean flow and distribution of large-scale weather systems in the southern hemisphere: The effects of moisture transports, *Q. J. R Meteorol. Soc., 110*, 943-966, 1983.

Johnson, W. B., and W. Viezee, Stratospheric ozone in the lower troposphere, 1, Presentation and interpretation of aircraft measurements, *Atmos. Env., 15*, 1309-1323, 1981.

Kalvova, J., and T. Halenka, On the relation between circulation and total ozone value extremes, *Ann. Geophys., 13*, suppl., C717, 1995.

Koike, M., et al., Reactive nitrogen and its correlation with O_3 and CO over the Pacific in winter and early spring, *J. Geophys. Res., 102*, 28,385-28,404, 1997.

Merrill, J. T., Trajectory results and interpretation for PEM-West A, *J. Geophys. Res., 101*, 1679-1690, 1996.

Monks, P. S., L. J. Carpenter, S. A. Penkett, G. P. Ayers, R. W. Gillett, I. E. Galbally, and C. P. Meyer, Fundamental ozone photochemistry in the remote marine boundary layer: The SOAPEX Experiment, measurement and theory, *Atmos. Environ., 32*, 3647-3664, 1998.

Newell, R. E., E. V. Browell, D. D. Davis, and S. C. Liu, Western Pacific tropospheric ozone and potential vorticity: Implications for Asian pollution, *Geophys. Res. Lett., 24*, 2733-2736, 1997.

Oltmans, S. J., et al., Summer and spring ozone profiles over the North Atlantic from ozonesonde measurements, *J. Geophys. Res., 101*, 29,179-29,200, 1996.

Pierce, R. B., and W. B. Grant, Seasonal evolution of Rossby and gravity wave induced laminae in ozonesonde data obtained from Wallops Island, Virginia, *Geophys. Res. Lett., 25*, 1859-1862, 1998.

Richter, D. A., E. V. Browell, C. F. Butler, and N. S. Higdon, Advanced airborne UV DIAL system for stratospheric and tropospheric ozone and aerosol measurements, in *Advances in Atmospheric Remote Sensing with Lidar*, edited by A. Ansmann, R. Neuber, P. Rairoux, and U. Wandinger, pp. 395-398, Springer-Verlag, New York, 1997.

Routhier, F., R. Dennett, D. D. Davis, A. Wartburg, P. Haagenson, and A. C. Delany, Free tropospheric and boundary layer airborne measurements of ozone over the latitude range of 58°S and 70°N, *J. Geophys. Res., 85*, 7307-7321, 1980.

Simpson, L. J., et al., Nonmethane hydrocarbon measurements in the North Atlantic flight corridor during SONEX, *J. Geophys. Res.*, this issue.

Singh, H. B., et al., Low ozone in the marine boundary layer of the tropical Pacific Ocean: Photochemical loss, chlorine atoms, and entrainment, *J. Geophys. Res., 101*, 1907-1917, 1996.

Singh, H. B., A. Thompson, and H. Schlager, SONEX airborne mission and coordinated POLINAT 2 activity: Overview and accomplishments,*Geophys. Res. Lett., 26*, 3053-3056, 1999.

Talbot, R. W., et al., Chemical characteristics of continental outflow over the tropical South Atlantic Ocean from Brazil and Africa, *J. Geophys. Res., 101*, 24,187-24,202, 1996.

Thompson, A. M., et al., Ozone observations and a model of marine boundary layer photochemistry during SAGA 3, *J. Geophys. Res., 98*, 16,955-16,968, 1993.

Thompson, A. M., L. C. Sparling, Y. Kondo, B. E. Anderson, G. L. Gregory, and G. W. Sachse, Perspectives on NO, NO_y and fine aerosol sources and variability during SONEX, *Geophys. Res. Lett., 26*, 3073-3076, 1999.

Thouret, V., A. Marenco, J. A. Logan, P. Nédélec, and C. Grouhel, Comparisons of ozone measurements from the MOZAIC airborne program and the ozone sounding network at eight locations, *J. Geophys. Res.*, *103*, 25,695-25,720, 1998.

Tsutsumi, Y., Y. Igarashi, Y. Zaizen, and Y. Makino, Case studies of tropospheric ozone events observed at the summit of Mount Fuji, *J. Geophys. Res.*, *103*, 16,935-16,951, 1998.

D. R. Blake and N. J. Blake, Chemistry Department, University of California, Irvine, CA 92717.

E. V. Browell, W. B. Grant, and G. L. Gregory, Atmospheric Sciences Research, NASA Langley Research Center, Hampton, VA 23681-0001 (w.b.grant@larc.nasa.gov).

C. F. Butler, M. B. Clayton, and M. A. Fenn, Science Applications International Corporation, NASA Langley Research Center, Hampton, VA 23681-0001.

H. E. Fuelberg and J. R. Hannan, Department of Meteorology, Florida State University, Tallahassee, FL 32306.

B. G. Heikes and J. Snow, Center for Atmospheric Chemistry Studies, Graduate School of Oceanography, University of Rhode Island, Narragansett, RI 02882.

G. W. Sachse, Aerospace Electronic Systems, NASA Langley Research Center, Hampton, VA 23681-0001.

H. B. Singh, NASA Ames Reserch Center, Moffett Field, CA 94035.

R. W. Talbot, Institute for the Study of Earth, Oceans, and Space, University of New Hampshire, Durham,NH 03824.

(Received April 5, 1999; revised September 28, 1999; accepted September 30, 1999.)